nature ecology & evolution

SUPPLEMENTARY INFORMATION
https://doi.org/10.1038/s41559-019-0924-0

In the format provided by the authors and unedited.

Climate change and cultural resilience in late pre-Columbian Amazonia

Jonas Gregorio de Souza[1,2*], Mark Robinson[2], S. Yoshi Maezumi[2,3], José Capriles[4], Julie A. Hoggarth[5], Umberto Lombardo[6], Valdir Felipe Novello[7], James Apaéstegui[8], Bronwen Whitney[9], Dunia Urrego[2], Daiana Travassos Alves[2], Stephen Rostain[10], Mitchell J. Power[11], Francis E. Mayle[12], Francisco William da Cruz Jr[7], Henry Hooghiemstra[13] and José Iriarte[2]

[1]Department of Humanities, Universitat Pompeu Fabra, Barcelona, Spain. [2]Department of Archaeology, University of Exeter, Exeter, UK. [3]Department of Geography and Geology, The University of the West Indies at Mona, Kingston, Jamaica. [4]Department of Anthropology, Pennsylvania State University, University Park, PA, USA. [5]Department of Anthropology, Baylor University, Waco, TX, USA. [6]Institute of Geography, Universität Bern, Bern, Switzerland. [7]Institute of Geoscience, Universidade de São Paulo, São Paulo, Brazil. [8]Instituto Geofísico del Peru, Lima, Peru. [9]Department of Geography and Environmental Sciences, Northumbria University, Newcastle, UK. [10]Department of Archaeology, French National Centre for Scientific Research, Paris, France. [11]Geography Department, The University of Utah, Salt Lake City, UT, USA. [12]Department of Geography and Environmental Science, University of Reading, Reading, UK. [13]Institute for Biodiversity and Ecosystem Dynamics, Universiteit van Amsterdam, Amsterdam, the Netherlands.
*e-mail: jonas.gregorio@gmail.com

Supplementary Information for

"Climate change and cultural resilience in late pre-Columbian Amazonia"

Jonas Gregorio de Souza, Mark Robinson, S. Yoshi Maezumi, José Capriles, Julie A. Hoggarth, Umberto Lombardo, Valdir Felipe Novello, James Apaéstegui, Bronwen Whitney, Dunia Urrego, Daiana Travassos Alves, Stephen Rostain, Mitchell J. Power, Francisco William da Cruz Jr., Francis E. Mayle, Henry Hooghiemstra, José Iriarte

Supplementary Discussion 1

For a long time, the classification of archaeological cultures in tropical lowland South America has been based on technological and stylistic attributes of the ceramics. Although the direct correlation between ceramic phases/traditions and different ethnic groups is not always demonstrable, recent reappraisals have reinforced the significance of concomitant changes in ceramics and settlement patterns for mapping actual peoples' movements in pre-Columbian Amazonia[1]. In what follows, we summarise the main attributes of the ceramic assemblages for each relevant culture discussed in the main text, where the reader can find detailed information about the respective settlement patterns and land use.

Arauquinoid: The Arauquinoid tradition, which rapidly spread from the Apure-Orinoco confluence to the Guianas, is a manifestation of the broader Amazonian Incised-Punctate Tradition. The first period of the Arauquinoid tradition, represented by the Hertenrits style, is marked by pottery with simple decoration, such rim incisions and wavy applied clay fillets. Pottery becomes more diversified over time, with incised, punctate and applied designs, as well as clay figurines. The later Kwatta style has more elaborate ceramics, with rows of incisions, red painting, zoomorphic adornments and anthropomorphic faces, also specialising in the production of *muiraquitãs* (zoomorphic green stone pendants). Finally, the Barbakoeba style of Arauquinoid pottery is the coarser, with applied motifs, incisions, fingertip impressions and anthropomorphic faces as adornments[2].

Koriabo: The Koriabo tradition, the "only truly Guianas cultural style that is not found out of this area"[2], has its earliest manifestations inland, later moving to the coast. Vessel shapes and incised designs in Koriabo pottery are homogeneous throughout its territory. Decoration includes fine incisions, wide and shallow incisions, modelled zoomorphic motifs, human faces and some painting in white, red and black[2].

Marajoara: The prestige ceramics, in particular the funerary urns, associated with the Marajoara phase are one of the most iconic styles of pre-Columbian Amazonia. Although often included in the broader Polychrome tradition, Marajoara pottery appears to be a separate development. The prestige and ceremonial vessels of Joanes Painted style are profusely decorated with painted designs (red and black) on a white slipped surface. Painted motifs are curvilinear and geometric, forming anthropomorphic (heads, faces, legs) and zoomorphic (scorpions, snakes, vultures) features. Female figurines and *tangas* (pubic coverings) appear as part of the ceremonial apparatus alongside the funerary urns and other painted vessels[3].

Santarém: This ceramic phase, considered to be part of the broader Amazonian Incised-Punctate Tradition, is known for its complex modelled decorations. Caryatid and neck vessels are adorned with a myriad of geometric plastic and painted designs, combined with realistic zoomorphic and anthropomorphic appendages. Effigy vessels depict parts of animals like the agouti, king vulture, harpy eagle, caiman and jaguar, as well as human figures mixed with zoomorphic features. Small female and large male figurines are also present. As in the case of the Kwatta Arauquinoid sites, *Muiraquitãs* (zoomorphic green stone pendants) are part of the Santarém cultural package[4,5].

Paredão: The ceramics of the Paredão phase appear to be a local development of Central Amazon, where they emerged out of complexes related to the broader Incised Rim Tradition. Paredão pottery is very thin and well fired, tempered with *cauixi* (sponge spicules). Some vessels exhibit handles and pedestals. Decoration includes fine incisions and painting, as well as red slip. Funerary urns associated with this phase are recognisable by the presence of modelled anthropomorphic appendages, including stylised heads[6].

Guarita: The Guarita phase is the manifestation, in Central Amazon, of the nearly pan-Amazonian Polychrome Tradition. Guarita ceramics are tempered with crushed potsherds and decorated with a profusion of bold and fine geometric motifs painted in red and black over a white-slipped surface. Plastic decoration with grooves forming the same geometric designs is also present. Vessels present thickened rims, mesial flanges, and include anthropomorphic funerary urns. As in the case of the Marajoara iconography, the painted motifs on Guarita ceramics can be read as stylised zoomorphic motifs (serpents, vultures) intertwined so as to convey anthropomorphic figures[6].

Geoglyphs: The ceramics associated with the period of construction of the Geoglyphs have been classified in the Quinari Tradition. Quinari ceramics are tempered with *caraipé* (tree bark) and charcoal, and most of the potsherds are very fragmented, plain and eroded, with eventual white and red slips. Vessels are cylindrical or globular, also with angular shoulders. The most distinctive type of Quinari ceramics are anthropomorphic jars representing human faces, although their direct association with the Geoglyphs is uncertain. Other decorated vessels are incised with angular, parallel, curved and spiral lines, forming concentric and interlocked designs[7,8].

Mound villages: The ceramics associated with the mound ring villages of Acre are generally cruder than the ceramics of the Geoglyphs[7]. Due to the fact that research in mound villages is still in its beginnings, little is known about their portable material culture, but preliminary data show other differences relative to the earlier ditches, such as the presence of red painted geometric designs on a white-slipped surface[9].

Lomas: The ceramics from the monumental mounds of the Llanos de Moxos have been assigned to the Casarabe Tradition, which encompasses five phases. Phase 1 is characterised by bowls with red painted triangular designs and parallel lines. Phase 2 has fewer decorated bowls, with predominance of incised lines and punctuations. In Phase 3, bowls become closer, with triangular and spiral incisions, accompanied by jars with deeply incised triangles and wavy lines near the rim. Phase 4 is characterised by open bowls with painted decoration, forming horizontal or diagonal bands surrounded by dots or wavy lines. Bowls with angular shoulders also appear, painted with complex motifs combining fine triangles, concentric curves, wavy bands and other designs. Finally, Phase 5 has open dishes painted with fine lines forming steps, spirals and other patterns, together with hexagonal jars decorated with painted bands[10].

Zanjas: The ceramics from the ring ditches in the Llanos de Moxos have been assigned to the Irobi Phase. They are characterised by small necked jars and bowls with fine incised bands, steps, parallel lines, spirals, concentric lines, hachured triangles and other designs. Controlled firing was used in some jars to create a bicolour effect (black and orange) due to differential oxidation. This heavily decorated, high quality pottery seems to be present especially in funerary contexts[11].

Xinguano: The ceramics from the Upper Xingu earthworks belong to the Ipavu Phase, part of the broader Barrancoid horizon in Amazonia, with influences from the Incised-Punctate and Polychrome Traditions. Like other Barrancoid styles, Ipavu ceramics are characterised by modelled appendages, incised lines forming parallel and curvilinear patterns, and red slip. Archaeological ceramics show remarkable similarity with the ones still manufactured by Upper Xingu peoples today. Ceramics were formed by the paddle-and-anvil technique and tempered with *cauixi* (sponge spicules) and *caraipé* (tree bark). The assemblage is composed of open and flat-bottomed vessels, constricted jars, and griddles. Modern Xinguano ceramics differ from archaeological ones by the inclusion of zoned red slip, black painted designs and exterior white slip[12].

Supplementary Discussion 2

In the main text, we have noticed that the climate systems impacting Amazonia create a precipitation dipole at the borders of the South American Summer Monsoon, resulting in a climatic antiphase between western and eastern Amazon Basin. Here, those concepts are explained in greater detail.

The ITCZ is characterised by a tropical belt of deep convective clouds that provide a high amount of precipitation[13,14]. Seasonally, the ITCZ migrates towards the hemisphere that is warmest relative to the other. At present climatology, over the Americas, the ITCZ migrates from approximately 9°N in the austral winter to approximately 2°S in the austral summer. However, a positioning of the ITCZ further south has been documented by palaeoclimate records[15]. The SASM is the main convective system over South America, and its intensity is closely related to the position of the ITCZ, with southward migrations of the ITCZ increasing the advective moisture carried by the SASM. During the austral summer, the South American continent experiences warmer conditions relative to the Atlantic Ocean, which favours the entry of moisture into the continent in association with the southward displacement of the ITCZ, ultimately resulting in a wet monsoonal season.

High convection over the SASM domain is also associated with the formation of the South Atlantic Convergence Zone (SACZ), which is an internal structure of the SASM characterised by a NW-SE band of convection that extends from the centre of convection to eastern Brazil. As the ITCZ, the SACZ migrates, though in a SW-NE axis due to the adjustment of atmospheric cells over the continent. The migration of the SACZ creates a rainfall dipole at the borders of the monsoon, resulting in a climatic antiphase between western and eastern Amazon Basin[16].

Supplementary Note

Calibration of the dates in Supplementary Table 1 was performed in OxCal 4.2[17]. Because all the sites are in regions affected by the SASM (see main text), dates have been calibrated with mixed IntCal13[18] and ShCal13[19] curves following Marsh et al[20]. Sites with multiple dates and cultural components were modelled as sequences with separate phases and simple boundaries delimiting the start and end of each phase[21]. Outliers (marked in red with * in the tables) were identified based on a 60% agreement threshold and removed from subsequent runs of the models.

Supplementary Table 1. Radiocarbon dates for Arauquinoid and Koriabo sites in the Guianas Coast.

Guianas coast					
Site	Date (RCYBP)	cal CE (2σ)	Laboratory#	Phase	Reference
Angouleme	440 ± 30	1430-1615	LY-4949	Koriabo	(Van den Bel, 2015)[22]
Bigiston	410 ± 60	1430-1635	GrN-4240	Koriabo	(Rostain, 1994)[23]
Blauwgrond II	520 ± 50	1315-1480	GrN-2173	Koriabo	(Rostain, 1994)[23]
Bois Diable	750 ± 40	1215-1385	Beta-254054	Arauquinoid	(McKey et al., 2010)[24]
Christiaankondre	440 ± 50	1415-1630	GrN-4241	Koriabo	(Rostain, 1994)[23]
Coroeni Island	785 ± 50	1170-1375	GrN-2174	Koriabo	(Rostain, 1994)[23]
Crique Sparouine	1045 ± 20	985-1030	KIA-33555	Koriabo	(Van den Bel, 2010)[25]
Crique Sparouine	905 ± 26	1045-1220	KIA-32395	Koriabo	(Van den Bel, 2010)[25]
Crique Sparouine	747 ± 25	1230-1300	KIA-32396	Koriabo	(Van den Bel, 2010)[25]
Crique Sparouine	585 ± 25	1310-1420	KIA-32394	Koriabo	(Van den Bel, 2010)[25]
Hertenrits-Wageningen	1310 ± 30	680-875	GrN-10301	Arauquinoid	(Rostain, 1994)[23]
Hertenrits-Wageningen	1265 ± 60	685-940	GrN-1897	Arauquinoid	(Rouse and Allaire, 1978)[26]
Hertenrits-Wageningen	1245 ± 25	725-885	GrN-9061	Arauquinoid	(Rostain, 1994)[23]
Hertenrits-Wageningen	1240 ± 30	720-890	GrN-9359	Arauquinoid	(Rostain, 1994)[23]
Hertenrits-Wageningen	1230 ± 25	765-885	GrN-9060	Arauquinoid	(Rostain, 1994)[23]
Hertenrits-Wageningen	1210 ± 25	770-895	GrN-9059	Arauquinoid	(Rouse and Allaire, 1978)[26]
Hertenrits-Wageningen	1145 ± 30	775-980	GrN-9360	Arauquinoid	(Rostain, 1994)[23]
Hertenrits-Wageningen	1130 ± 60	770-980	GrN-845c	Arauquinoid	(Rostain, 1994)[23]
Hertenrits-Wageningen	1130 ± 45	775-980	GrN-1898	Arauquinoid	(Rostain, 1994)[23]
K-VIII	1010 ± 40	990-1155	Beta-254058	Arauquinoid	(McKey et al., 2010)[24]
Morico Creek	455 ± 65	1400-1630	GrN-2321	Koriabo	(Rostain, 1994)[23]
Peruvia	1210 ± 30	770-960	GrN-9361	Arauquinoid	(Rostain, 1994)[23]
Peruvia	755 ± 35	1220-1375	GrN-9800	Arauquinoid	(Rostain, 1994)[23]
Prins Bernhard Polder	1335 ± 38	645-835	GrN-8955	Arauquinoid	(Rostain, 1994)[23]
Prins Bernhard Polder	935 ± 50	1025-1220	GrN-8954	Arauquinoid	(Rostain, 1994)[23]
Prins Bernhard Polder	790 ± 25	1220-1280	GrN-9801	Arauquinoid	(Rostain, 1994)[23]
Sable Blanc	990 ± 30	1025-1165	LY-4958	Arauquinoid	(McKey et al., 2010)[24]
Sable Blanc	955 ± 30	1040-1185	LY-4956	Arauquinoid	(McKey et al., 2010)[24]
Sable Blanc	925 ± 30	1050-1210	LY-4958	Arauquinoid	(McKey et al., 2010)[24]
Sable Blanc	920 ± 30	1050-1215	LY-4960	Arauquinoid	(McKey et al., 2010)[24]
Sable Blanc	900 ± 30	1050-1225	LY-4959	Arauquinoid	(McKey et al., 2010)[24]
Sable Blanc	880 ± 30	1055-1240	LY-4960	Arauquinoid	(McKey et al., 2010)[24]
Sable Blanc	825 ± 30	1155-1260	LY-4961	Arauquinoid	(McKey et al., 2010)[24]
Saut Saillat	425 ± 20	1440-1615	KIA-31240	Koriabo	(Van den Bel, 2015)[22]
Saut Saillat	390 ± 20	1450-1620	KIA-31242	Koriabo	(Van den Bel, 2015)[22]
Saut Saillat	360 ± 25	1455-1625	KIA-31239	Koriabo	(Van den Bel, 2015)[22]
Tingiholo	1140 ± 90	840-1155	GrN-8250	Arauquinoid	(Rostain, 1994)[23]
Tingiholo	1050 ± 100	885-1170	GrN-8249	Arauquinoid	(Rostain, 1994)[23]
Tingiholo	1025 ± 50	970-1155	GrN-12913	Arauquinoid	(Rostain, 1994)[23]
Tingiholo	970 ± 50	990-1160	GrN-4552	Arauquinoid	(Rostain, 1994)[23]

Supplementary Table 2. Radiocarbon dates for Marajoara and Santarém sites in Eastern Amazon.

Eastern Amazon					
Site	Date (RCYBP)	cal CE (2σ)	Laboratory#	Phase	Reference
Alvorada	680 ± 50	1270-1400	Beta-293282	Santarém	(Martins, 2012)[27]
Amapá	300 ± 30	1500-1665	Beta-324176	Santarém	(Schaan, 2016)[5]
Camutins	1300 ± 40	680-885	Beta-160716	Marajoara	(Schaan, 2004)[28]
Camutins	1290 ± 60	675-945	Beta-134538	Marajoara	(Schaan, 2004)[28]
Camutins	1250 ± 60	695-960	Beta-179075	Marajoara	(Schaan, 2004)[28]
Camutins	1200 ± 60	720-990	Beta-180942	Marajoara	(Schaan, 2004)[28]
Camutins	1190 ± 40	770-965	Beta-185013	Marajoara	(Schaan, 2004)[28]
Camutins	1140 ± 40	775-995	Beta-134537	Marajoara	(Schaan, 2004)[28]
Camutins	1140 ± 60	775-1000	Beta-160717	Marajoara	(Schaan, 2004)[28]
Camutins	1060 ± 40	885-1030	Beta-188991	Marajoara	(Schaan, 2004)[28]
Cedro	550 ± 30	1325-1445	Beta-324192	Santarém	(Schaan, 2016)[5]
Cedro	240 ± 30	1525-1950	Beta-324193	Santarém	(Schaan, 2016)[5]
Bom Futuro	586 ± 30	1320-1435	Ua-46306	Santarém	(Schaan, 2016)[5]
Bom Futuro	540 ± 30	1395-1445	Ua-46305	Santarém	(Schaan, 2016)[5]
Bom Futuro	497 ± 30	1405-1455	Ua-46304	Santarém	(Schaan, 2016)[5]
Bom Futuro	350 ± 30	1450-1625	Beta-324178	Santarém	(Schaan, 2016)[5]
Fazenda Cacau	460 ± 30	1415-1490	Beta-293286	Santarém	(Martins, 2012)[27]
Guajará	1335 ± 185	480-1180	GX-16061	Marajoara	(Roosevelt, 1991)[29]
Guajará	1060 ± 50	890-1150	GX-16063	Marajoara	(Roosevelt, 1991)[29]
Guajará	675 ± 165	900-1460	GX-16061	Marajoara	(Roosevelt, 1991)[29]
PA-JO-36	1470 ± 200	240-980	SI-386	Marajoara	(Meggers and Danon, 1988)[30]
PA-JO-36	1370 ± 200	260-1025	SI-387	Marajoara	(Meggers and Danon, 1988)[30]
Porto	3830 ± 30	2345-2135 BCE	Beta-388953	Pocó	(Maezumi et al., 2018)[31]
Porto	3530 ± 30	1920-1745 BCE	Beta-388955	Pocó	(Maezumi et al., 2018)[31]
Porto	3260 ± 30	1610-1435 BCE	Beta-322223	Pocó	(Alves, 2012)[32]
Porto	3070 ± 30	1405-1220 BCE	Beta-386143	Pocó	(Maezumi et al., 2018)[31]
Porto	3060 ± 30	1400-1210 BCE	Beta-322221	Pocó	(Alves, 2012)[32]
Porto	3050 ± 30	1400-1130 BCE	Beta-386145	Pocó	(Maezumi et al., 2018)[31]
Porto	3030 ± 30	1385-1125 BCE	Beta-388950	Pocó	(Maezumi et al., 2018)[31]
Porto	3030 ± 30	1385-1125 BCE	Beta-388954	Pocó	(Maezumi et al., 2018)[31]
Porto	2912 ± 56	1230-915 BCE	WK6836	Pocó	(Quinn, 2004)[33]
Porto	2900 ± 30	1195-935 BCE	Beta-322219	Pocó	(Alves, 2012)[32]
Porto	2820 ± 30	1025-845 BCE	Beta-386138	Pocó	(Maezumi et al., 2018)[31]
Porto	2270 ± 63	415-140 BCE	WK6834	Pocó	(Quinn, 2004)[33]
Porto	1550 ± 30	430-600	Beta-386144	Pocó	(Maezumi et al., 2018)[31]
Porto	1260 ± 30	680-880	Beta-386139	Pocó	(Maezumi et al., 2018)[31]
Porto	1210 ± 30	765-960	Beta-388952	Pocó	(Maezumi et al., 2018)[31]
Porto	1140 ± 30	780-995	Beta-386135	Pocó	(Maezumi et al., 2018)[31]
Porto	960 ± 30*	1025-1165	Beta-322202	Santarém	(Alves, 2012)[32]
Porto	664 ± 57	1325-1425	WK6844	Santarém	(Quinn, 2004)[33]
Porto	660 ± 30	1315-1405	Beta-386141	Santarém	(Maezumi et al., 2018)[31]
Porto	652 ± 56	1325-1430	WK6837	Santarém	(Quinn, 2004)[33]

Porto	650 ± 59	1325-1430	WK6843	Santarém	(Quinn, 2004)[33]
Porto	640 ± 30	1325-1410	Beta-386134	Santarém	(Maezumi et al., 2018)[31]
Porto	590 ± 30	1320-1430	Beta-386136	Santarém	(Maezumi et al., 2018)[31]
Porto	586 ± 56	1325-1445	WK6839	Santarém	(Quinn, 2004)[33]
Porto	583 ± 57	1330-1445	WK6833	Santarém	(Quinn, 2004)[33]
Porto	537 ± 58	1325-1470	WK6840	Santarém	(Quinn, 2004)[33]
Porto	512 ± 59	1335-1490	WK6846	Santarém	(Quinn, 2004)[33]
Porto	500 ± 30	1405-1455	Beta-386140	Santarém	(Maezumi et al., 2018)[31]
Porto	490 ± 30	1410-1460	Beta-386148	Santarém	(Maezumi et al., 2018)[31]
Porto	460 ± 30	1420-1485	Beta-386142	Santarém	(Maezumi et al., 2018)[31]
Porto	455 ± 63	1400-1505	WK6845	Santarém	(Quinn, 2004)[33]
Porto	452 ± 57	1405-1500	Wk6837	Santarém	(Quinn, 2004)[33]
Porto	425 ± 56	1415-1505	WK6841	Santarém	(Quinn, 2004)[33]
Porto	418 ± 59	1415-1510	WK6842	Santarém	(Quinn, 2004)[33]
Porto	413 ± 56	1420-1510	WK6838	Santarém	(Quinn, 2004)[33]
Porto	410 ± 30	1440-1500	Beta-386146	Santarém	(Maezumi et al., 2018)[31]
Porto	400 ± 30	1445-1505	Beta-386147	Santarém	(Maezumi et al., 2018)[31]
Porto	400 ± 30	1445-1505	Beta-388951	Santarém	(Maezumi et al., 2018)[31]
Porto	386 ± 62	1425-1515	WK6832	Santarém	(Quinn, 2004)[33]
Porto	380 ± 64	1425-1515	WK6835	Santarém	(Quinn, 2004)[33]
Serra do Maguari	470 ± 30	1420-1495	Beta-433637	Santarém	(Maezumi et al., 2018)[31]
Serra do Maguari	430 ± 30	1435-1615	Beta-433632	Santarém	(Maezumi et al., 2018)[31]
Serra do Maguari	390 ± 30	1445-1620	Beta-433631	Santarém	(Maezumi et al., 2018)[31]
Serra do Maguari	390 ± 30	1445-1620	Beta-433630	Santarém	(Maezumi et al., 2018)[31]
Serra do Maguari	380 ± 30	1450-1620	Beta-433629	Santarém	(Maezumi et al., 2018)[31]
Serra do Maguari	330 ± 30	1475-1640	Beta-433635	Santarém	(Maezumi et al., 2018)[31]
Serra do Maguari	300 ± 30	1490-1650	Beta-433634	Santarém	(Maezumi et al., 2018)[31]
Serra do Maguari	290 ± 30	1495-1660	Beta-433628	Santarém	(Maezumi et al., 2018)[31]
Serraria Trombetas	890 ± 30	1050-1265	Beta-293289	Santarém	(Martins, 2012)[27]
Serraria Trombetas	780 ± 30	1220-1290	Beta-324188	Santarém	(Martins, 2012)[27]
Serraria Trombetas	580 ± 30	1305-1430	Beta-324187	Santarém	(Martins, 2012)[27]
Teso dos Bichos	2020 ± 280*	760 BCE-560 CE	SI-202	Marajoara	(Roosevelt, 1991)[29]
Teso dos Bichos	1260 ± 200	835-1125	SI-199	Marajoara	(Roosevelt, 1991)[29]
Teso dos Bichos	1225 ± 165	835-1120	GX-16075	Marajoara	(Roosevelt, 1991)[29]
Teso dos Bichos	1210 ± 50	840-1020	GX-16068	Marajoara	(Roosevelt, 1991)[29]
Teso dos Bichos	1120 ± 60	875-1035	GX-16076	Marajoara	(Roosevelt, 1991)[29]
Teso dos Bichos	1110 ± 60	880-1040	GX-16069	Marajoara	(Roosevelt, 1991)[29]
Teso dos Bichos	1080 ± 50	890-1045	GX-16067	Marajoara	(Roosevelt, 1991)[29]
Teso dos Bichos	1075 ± 290	855-1160	GX-10006	Marajoara	(Roosevelt, 1991)[29]
Teso dos Bichos	1030 ± 75	895-1135	GX-16065	Marajoara	(Roosevelt, 1991)[29]
Teso dos Bichos	1000 ± 90	900-1150	GX-16071	Marajoara	(Roosevelt, 1991)[29]
Teso dos Bichos	955 ± 195	875-1165	GX-12516	Marajoara	(Roosevelt, 1991)[29]
Teso dos Bichos	955 ± 220	870-1165	GX-12517	Marajoara	(Roosevelt, 1991)[29]
Teso dos Bichos	930 ± 190	880-1170	GX-12515	Marajoara	(Roosevelt, 1991)[29]
Teso dos Bichos	925 ± 75	965-1180	GX-16070	Marajoara	(Roosevelt, 1991)[29]
Teso dos Bichos	860 ± 110	905-1190	GX-16064	Marajoara	(Roosevelt, 1991)[29]

Teso dos Bichos	755 ± 160*	900-1475	GX-10005	Marajoara	(Roosevelt, 1991)[29]
Teso dos Bichos	755 ± 110*	1040-1415	GX-16066	Marajoara	(Roosevelt, 1991)[29]
Teso dos Bichos	550 ± 500	860-1170	SI-200	Marajoara	(Roosevelt, 1991)[29]
Teso dos Bichos	525 ± 385	1045-1950	GX-10004	Teso	(Roosevelt, 1991)[29]

Supplementary Table 3. Radiocarbon dates for Paredão and Guarita sites in the Central Amazon.

Central Amazon					
Site	Date (RCYBP)	cal CE (2σ)	Laboratory#	Phase	Reference
Açutuba	1590 ± 60	420-645	Beta-106438	Manacapuru	(Heckenberger et al., 1999)[34]
Açutuba	1270 ± 60	655-945	Beta-90723	Manacapuru	(Heckenberger et al., 1999)[34]
Açutuba	1230 ± 70	675-970	Beta-106437	Manacapuru	(Heckenberger et al., 1999)[34]
Açutuba	1100 ± 60	775-1035	Beta-109182	Manacapuru	(Heckenberger et al., 1999)[34]
Açutuba	1030 ± 100	765-1155	Beta-97527	Manacapuru	(Heckenberger et al., 1999)[34]
Açutuba	980 ± 60*	985-1210	Beta-90009	Guarita	(Heckenberger et al., 1999)[34]
Açutuba	790 ± 40	1220-1380	Beta-97529	Guarita	(Heckenberger et al., 1999)[34]
Açutuba	710 ± 80	1235-1405	Beta-109180	Guarita	(Heckenberger et al., 1999)[34]
Açutuba	690 ± 40	1270-1395	Beta-97530	Guarita	(Heckenberger et al., 1999)[34]
Açutuba	670 ± 60	1270-1405	Beta-109184	Guarita	(Heckenberger et al., 1999)[34]
Açutuba	600 ± 80	1275-1430	Beta-109178	Guarita	(Heckenberger et al., 1999)[34]
Açutuba	520 ± 80	1285-1450	Beta-109181	Guarita	(Heckenberger et al., 1999)[34]
Açutuba	510 ± 70	1290-1455	Beta-109183	Guarita	(Heckenberger et al., 1999)[34]
Antônio Galo	1216 ± 27	765-950	OxA-15505	Paredão	(Moraes, 2006)[35]
Antônio Galo	930 ± 30	1030-1195	Beta-297120	Paredão	(Moraes, 2013)[36]
Antônio Galo	190 ± 30*	1655-1950	Beta-297122	Guarita	(Moraes, 2013)[36]
Hatahara	1580 ± 40	425-630	Beta-145483	Manacapuru	(Arroyo-Kalin, 2009)
Hatahara	1390 ± 40	595-765	Beta-145484	Manacapuru	(Arroyo-Kalin, 2009)[37]
Hatahara	1300 ± 40	650-825	Beta-143599	Manacapuru	(Machado, 2005)[38]
Hatahara	1110 ± 40*	885-1025	Beta-143598	Manacapuru	(Machado, 2005)[38]
Hatahara	1250 ± 70*	660-970	Beta-143584	Paredão	(Machado, 2005)[38]
Hatahara	1250 ± 80*	660-975	Beta-143591	Paredão	(Machado, 2005)[38]
Hatahara	1150 ± 40	910-1025	Beta-178916	Paredão	(Machado, 2005)[38]
Hatahara	1130 ± 40	910-1025	Beta-145486	Paredão	(Arroyo-Kalin, 2009)[37]
Hatahara	1070 ± 50	905-1130	Beta-143593	Paredão	(Machado, 2005)[38]
Hatahara	1010 ± 80	950-1165	Beta-143583	Paredão	(Machado, 2005)[38]
Hatahara	1000 ± 40	995-1150	Beta-143588	Paredão	(Machado, 2005)[38]
Hatahara	1000 ± 40	995-1150	Beta-143589	Paredão	(Machado, 2005)[38]
Hatahara	980 ± 40	1010-1155	Beta-242439	Paredão	(Prestes-Carneiro et al., 2016)[39]
Hatahara	980 ± 40	1010-1155	Beta-143585	Paredão	(Machado, 2005)[38]
Hatahara	970 ± 40	1015-1155	Beta-178914	Paredão	(Machado, 2005)[38]
Hatahara	960 ± 30	1025-1155	Beta-143586	Paredão	(Machado, 2005)[38]
Hatahara	920 ± 40	1025-1175	Beta-143592	Paredão	(Machado, 2005)[38]
Hatahara	910 ± 40	1030-1180	Beta-178915	Paredão	(Machado, 2005)[38]
Hatahara	570 ± 40	1315-1445	Beta-143587	Guarita	(Machado, 2005)[38]
Hatahara	350 ± 40	1450-1630	Beta-143582	Guarita	(Machado, 2005)[38]
Lago Grande	1260 ± 40*	680-885	Beta-143606	Paredão	(Neves and Petersen, 2006)[40]

Lago Grande	1180 ± 40	875-995	Beta-178923	Paredão	(Neves and Petersen, 2006)[40]
Lago Grande	1150 ± 40	890-1015	Beta-143603	Paredão	(Neves and Petersen, 2006)[40]
Lago Grande	1130 ± 40	900-1020	Beta-143604	Paredão	(Neves and Petersen, 2006)[40]
Lago Grande	1110 ± 40	900-1025	Beta-178927	Paredão	(Neves and Petersen, 2006)[40]
Lago Grande	1110 ± 40	900-1025	Beta-178922	Paredão	(Neves and Petersen, 2006)[40]
Lago Grande	1100 ± 30	900-1025	Beta-143605	Paredão	(Neves and Petersen, 2006)[40]
Lago Grande	1050 ± 40	900-1125	Beta-178925	Paredão	(Neves and Petersen, 2006)[40]
Lago Grande	1050 ± 40	900-1120	Beta-143600	Paredão	(Neves and Petersen, 2006)[40]
Lago Grande	960 ± 40	1015-1145	Beta-178921	Paredão	(Neves and Petersen, 2006)[40]
Lago Grande	960 ± 30	1020-1140	Beta-143607	Paredão	(Neves and Petersen, 2006)[40]
Lago Grande	950 ± 60	990-1145	Beta-178919	Paredão	(Neves and Petersen, 2006)[40]
Lago Grande	950 ± 40	1020-1145	Beta-143601	Paredão	(Neves and Petersen, 2006)[40]
Lago Grande	950 ± 30	1025-1140	Beta-143602	Paredão	(Neves and Petersen, 2006)[40]
Lago do Limão	1660 ± 28	355-530	OxA-15502	Manacapuru	(Moraes, 2006)[35]
Lago do Limão	846 ± 27	1165-1265	OxA-15503	Paredão	(Moraes, 2006)[35]
Lago do Limão	625 ± 26	1300-1405	OxA-15504	Guarita	(Moraes, 2006)[35]
Osvaldo	1350 ± 40	670-770	Beta-143627	Manacapuru	(Moraes, 2006)[35]
Osvaldo	1340 ± 40	670-770	Beta-143617	Manacapuru	(Moraes, 2006)[35]
Osvaldo	1330 ± 40	670-770	Beta-143612	Manacapuru	(Moraes, 2006)[35]
Osvaldo	1320 ± 60	670-770	Beta-143619	Manacapuru	(Moraes, 2006)[35]
Osvaldo	1310 ± 40	675-770	Beta-143620	Manacapuru	(Moraes, 2006)[35]
Osvaldo	1290 ± 30	680-770	Beta-143609	Manacapuru	(Moraes, 2006)[35]
Osvaldo	1290 ± 40	675-770	Beta-143613	Manacapuru	(Moraes, 2006)[35]
Osvaldo	1260 ± 30	680-775	Beta-143623	Manacapuru	(Moraes, 2006)[35]
Osvaldo	1216 ± 27*	765-945	OxA-15505	Manacapuru	(Moraes, 2006)[35]
Osvaldo	1100 ± 40*	890-1025	Beta-143626	Manacapuru	(Moraes, 2006)[35]
Osvaldo	930 ± 30	1045-1215	Beta-297120	Paredão	(Moraes, 2006)[35]
Osvaldo	846 ± 27	1155-1250	OxA-15503	Paredão	(Moraes, 2006)[35]
Osvaldo	725 ± 26	1265-1385	OxA-15504	Guarita	(Moraes, 2006)[35]
Osvaldo	190 ± 30*	1655-1950	Beta-297122	Guarita	(Moraes, 2006)[35]

Supplementary Table 4. Radiocarbon dates for Geoglyphs and Mound Ring Villages in Southwestern Amazon.

Southwestern Amazon					
Site	Date (RCYBP)	cal CE (2σ)	Laboratory#	Phase	Reference
Balneário Quinauá	1760 ± 35	245-410	Ua-37261	Geoglyph	(Saunaluoma and Schaan, 2012)[8]
Balneário Quinauá	1585 ± 30	415-555	Ua-37260	Geoglyph	(Saunaluoma and Schaan, 2012)[8]
Balneário Quinauá	1570 ± 35	415-575	Ua-37262	Geoglyph	(Saunaluoma and Schaan, 2012)[8]
Balneário Quinauá	1565 ± 35	420-580	Ua-37263	Geoglyph	(Saunaluoma and Schaan, 2012)[8]
Severino Calazans	2275 ± 35	400-200 BCE	Ua-37265	Geoglyph	(Schaan et al., 2012)[41]
Severino Calazans	2050 ± 35	155 BCE-50 CE	Ua-37264	Geoglyph	(Schaan et al., 2012)[41]

El Círculo	715 ± 30	1280-1390	Poz-9426	Mound village	(Saunaluoma, 2010)[9]
El Círculo	685 ± 30	1285-1390	Poz-9428	Mound village	(Saunaluoma, 2010)[9]
El Círculo	680 ± 30	1285-1390	Poz-9523	Mound village	(Saunaluoma, 2010)[9]
El Círculo	660 ± 30	1290-1395	Poz-9427	Mound village	(Saunaluoma, 2010)[9]
El Círculo	650 ± 30	1290-1395	Poz-9524	Mound village	(Saunaluoma, 2010)[9]
El Círculo	645 ± 30	1290-1395	Poz-9429	Mound village	(Saunaluoma, 2010)[9]
El Círculo	600 ± 60	1290-1395	Hela-4585	Mound village	(Saunaluoma, 2010)[9]
Fazenda Iquiri II	1741 ± 60	245-400	Ua-49945	Geoglyph	(Saunaluoma et al., 2018)[42]
Fazenda Iquiri II	706 ± 31	1265-1385	Ua-49946	Geoglyph	(Saunaluoma et al., 2018)[42]
Fazenda Iquiri II	476 ± 30	1410-1610	Ua-49944	Mound village	(Saunaluoma et al., 2018)[42]
Fazenda Iquiri II	285 ± 31	1495-1670	Ua-49943	Mound village	(Saunaluoma et al., 2018)[42]
Fazenda Atlântica	2110 ± 35	200 BCE-15 CE	Ua-37253	Geoglyph	(Saunaluoma and Schaan, 2012)[8]
Fazenda Atlântica	1905 ± 35	50-220	Ua-37251	Geoglyph	(Saunaluoma and Schaan, 2012)[8]
Fazenda Atlântica	1855 ± 30	85-245	Ua-37252	Geoglyph	(Saunaluoma and Schaan, 2012)[8]
Fazenda Colorada	1865 ± 65	65-355	Ua-37235	Geoglyph	(Schaan et al., 2012)[41]
Fazenda Colorada	1820 ± 30	130-335	Ua-37256	Geoglyph	(Schaan et al., 2012)[41]
Fazenda Colorada	1775 ± 35	210-385	Ua-37567	Geoglyph	(Schaan et al., 2012)[41]
Fazenda Colorada	1340 ± 35	650-770	Ua-37236	Geoglyph	(Schaan et al., 2012)[41]
Fazenda Colorada	1275 ± 30	675-850	Ua-37255	Geoglyph	(Schaan et al., 2012)[41]
Fazenda Colorada	750 ± 35	1220-1380	Hela-616	Mound village	(Schaan et al., 2012)[41]
JK	1830 ± 30	130-335	Beta-294310	Geoglyph	(Saunaluoma and Schaan, 2012)[8]
JK	1710 ± 30	245-410	Beta-294309	Geoglyph	(Saunaluoma and Schaan, 2012)[8]
Jacó Sá	1485 ± 35	550-650	Ua-37259	Geoglyph	(Schaan et al., 2012)[41]
Jacó Sá	1205 ± 30	765-955	Ua-37258	Geoglyph	(Schaan et al., 2012)[41]
Jacó Sá	1195 ± 30	765-955	Ua-37257	Geoglyph	(Schaan et al., 2012)[41]
Ramal do Capatará	1990 ± 30	45 BCE-115 CE	Beta-288233	Geoglyph	(Saunaluoma and Schaan, 2012)[8]
Ramal do Capatará	1850 ± 40	60-255	Beta-288232	Geoglyph	(Saunaluoma and Schaan, 2012)[8]
Sol de Campinas	960 ± 30	1030-1185	Beta-408408	Mound village	(Neves et al., 2016)[43]
Sol de Campinas	730 ± 30	1255-1385	Beta-408407	Mound village	(Neves et al., 2016)[43]
Sol de Campinas	660 ± 30	1285-1395	Beta-408409	Mound village	(Neves et al., 2016)[43]
Sol de Campinas	530 ± 30	1395-1450	Beta-408410	Mound village	(Neves et al., 2016)[43]
Sol de Campinas	440 ± 30	1425-1500	Beta-408412	Mound village	(Neves et al., 2016)[43]
Tequinho	1964 ± 40	35 BCE-135 CE	Ua-48321	Geoglyph	(Saunaluoma et al., 2018)[42]
Tequinho	1956 ± 34	5-135	Ua-48329	Geoglyph	(Saunaluoma et al., 2018)[42]

Tequinho	1879 ± 39	50-220	Ua-48323	Geoglyph	(Saunaluoma et al., 2018)[42]

Supplementary Table 5. Radiocarbon dates for *zanjas* (ring ditches) and *lomas* (mounds) in the Llanos de Moxos.

Llanos de Moxos					
Site	Date (RCYBP)	cal CE (2σ)	Laboratory #	Phase	Reference
Bella Vista	783 ± 25	1225-1285	KIA-48488	Zanja	(Prümers and Jaimes Betancourt, 2014)[11]
Bella Vista	782 ± 27	1225-1285	KIA-38831	Zanja	(Prümers and Jaimes Betancourt, 2014)[11]
Bella Vista	775 ± 25	1230-1290	KIA-48489	Zanja	(Prümers and Jaimes Betancourt, 2014)[11]
Bella Vista	726 ± 41	1240-1390	Erl-6558	Zanja	(Prümers and Jaimes Betancourt, 2014)[11]
Bella Vista	634 ± 44	1290-1410	Erl-6561	Zanja	(Prümers and Jaimes Betancourt, 2014)[11]
Bella Vista	607 ± 28	1300-1415	KIA-38833	Zanja	(Prümers and Jaimes Betancourt, 2014)[11]
Bella Vista	568 ± 43	1305-1445	Erl-6560	Zanja	(Prümers and Jaimes Betancourt, 2014)[11]
Bella Vista	470 ± 27	1415-1465	KIA-40611	Zanja	(Prümers and Jaimes Betancourt, 2014)[11]
Bella Vista	432 ± 18	1440-1480	KIA-40610	Zanja	(Prümers and Jaimes Betancourt, 2014)[11]
Jasiaquiri	610 ± 25	1315-1415	KIA-48482	Zanja	(Prümers and Jaimes Betancourt, 2014)[11]
Jasiaquiri	596 ± 25	1315-1420	KIA-48487	Zanja	(Prümers and Jaimes Betancourt, 2014)[11]
Jasiaquiri	500 ± 25	1410-1450	KIA-48484	Zanja	(Prümers and Jaimes Betancourt, 2014)[11]
Jasiaquiri	444 ± 25	1425-1480	KIA-48486	Zanja	(Prümers and Jaimes Betancourt, 2014)[11]
Loma Alta de Casarabe	1400 ± 75	580-870	SI-5371	Loma	(Dougherty and Calandra, 1984)[44]
Loma Alta de Casarabe	1375 ± 60	600-860	SI-5375	Loma	(Dougherty and Calandra, 1984)[44]
Loma Alta de Casarabe	1315 ± 70	640-895	SI-5372	Loma	(Dougherty and Calandra, 1984)[44]
Loma Alta de Casarabe	1140 ± 90	685-1125	SI-5384	Loma	(Dougherty and Calandra, 1984)[44]
Loma Alta de Casarabe	1060 ± 65	870-1165	SI-5382	Loma	(Dougherty and Calandra, 1984)[44]
Loma Alta de Casarabe	1055 ± 55	890-1155	SI-5870	Loma	(Dougherty and Calandra, 1984)[44]
Loma Alta de Casarabe	900 ± 70	1025-1265	SI-5380	Loma	(Dougherty and Calandra, 1984)[44]
Loma Alta de Casarabe	835 ± 70	1040-1290	SI-5381	Loma	(Dougherty and Calandra, 1984)[44]
Loma Alta de Casarabe	830 ± 70	1040-1295	SI-5383	Loma	(Dougherty and Calandra, 1984)
Loma Alta de Casarabe	755 ± 95	1045-1390	SI-5385	Loma	(Dougherty and Calandra, 1984)[44]
Loma Alta de Casarabe	680 ± 120	1040-1410	SI-5373	Loma	(Dougherty and Calandra, 1984)[44]
Loma Esperanza	1030 ± 45	965-1160	N/A	Loma	(Erickson, 2000)[45]
Loma Esperanza	600 ± 25	1305-1415	N/A	Loma	(Erickson, 2000)[45]

Loma Kiusiu	1355 ± 60	630-890	SI-4442	Loma	(Dougherty and Calandra, 1984)[44]
Loma Kiusiu	920 ± 70	1020-1265	SI-4438	Loma	(Dougherty and Calandra, 1984)[44]
Loma Kiusiu	895 ± 60	1035-1260	SI-4437	Loma	(Dougherty and Calandra, 1984)[44]
Loma Kiusiu	870 ± 70	1035-1275	SI-4440	Loma	(Dougherty and Calandra, 1984)[44]
Loma Kiusiu	820 ± 60	1045-1300	SI-4439	Loma	(Dougherty and Calandra, 1984)[44]
Loma Kiusiu	690 ± 65	1220-1400	SI-4436	Loma	(Dougherty and Calandra, 1984)[44]
Loma Mary	1360 ± 60	610-880	SI-4118	Loma	(Dougherty and Calandra, 1984)[44]
Loma Mary	970 ± 80	905-1260	SI-4116	Loma	(Dougherty and Calandra, 1984)[44]
Loma Mary	940 ± 70	995-1255	SI-4115	Loma	(Dougherty and Calandra, 1984)[44]
Loma Mary	640 ± 60	1275-1415	SI-4114	Loma	(Dougherty and Calandra, 1984)[44]
Loma Mendoza	1557 ± 39	515-640	Erl-4789	Loma	(Prümers and Jaimes Betancourt, 2014)[11]
Loma Mendoza	1512 ± 54	530-655	Erl-5613	Loma	(Prümers and Jaimes Betancourt, 2014)[11]
Loma Mendoza	1508 ± 51	535-655	Erl-5604	Loma	(Prümers and Jaimes Betancourt, 2014)[11]
Loma Mendoza	1465 ± 53	545-670	Erl-5606	Loma	(Prümers and Jaimes Betancourt, 2014)[11]
Loma Mendoza	1443 ± 38	575-670	Erl-4787	Loma	(Prümers and Jaimes Betancourt, 2014)[11]
Loma Mendoza	1417 ± 36	585-680	Erl-4790	Loma	(Prümers and Jaimes Betancourt, 2014)[11]
Loma Mendoza	1410 ± 53	570-770	Erl-5609	Loma	(Prümers and Jaimes Betancourt, 2014)[11]
Loma Mendoza	1407 ± 55	570-770	Erl-5608	Loma	(Prümers and Jaimes Betancourt, 2014)[11]
Loma Mendoza	1407 ± 52	575-770	Erl-5611	Loma	(Prümers and Jaimes Betancourt, 2014)[11]
Loma Mendoza	1371 ± 49	605-770	Erl-4786	Loma	(Prümers and Jaimes Betancourt, 2014)[11]
Loma Mendoza	1357 ± 51	600-835	Erl-5603	Loma	(Prümers and Jaimes Betancourt, 2014)[11]
Loma Mendoza	1342 ± 60	625-875	Erl-5607	Loma	(Prümers and Jaimes Betancourt, 2014)
Loma Mendoza	1338 ± 51	635-860	Erl-5605	Loma	(Prümers and Jaimes Betancourt, 2014)[11]
Loma Mendoza	1316 ± 57	645-875	Erl-5616	Loma	(Prümers and Jaimes Betancourt, 2014)[11]
Loma Mendoza	1313 ± 52	650-870	Erl-5612	Loma	(Prümers and Jaimes Betancourt, 2014)[11]
Loma Mendoza	1296 ± 36	660-860	Erl-4788	Loma	(Prümers and Jaimes Betancourt, 2014)[11]
Loma Mendoza	1254 ± 40	680-885	Erl-3207	Loma	(Prümers and Jaimes Betancourt, 2014)[11]
Loma Mendoza	1253 ± 36	680-885	Erl-3205	Loma	(Prümers and Jaimes Betancourt, 2014)[11]
Loma Mendoza	1238 ± 53	675-965	Erl-5615	Loma	(Prümers and Jaimes Betancourt, 2014)[11]
Loma Mendoza	1235 ± 53	675-965	Erl-5614	Loma	(Prümers and Jaimes Betancourt, 2014)[11]
Loma Mendoza	1231 ± 38	685-950	Erl-3206	Loma	(Prümers and Jaimes Betancourt, 2014)[11]
Loma Mendoza	1186 ± 66	685-1015	Erl-3202	Loma	(Prümers and Jaimes Betancourt, 2014)[11]

Loma Mendoza	1134 ± 33	880-1015	Bln-5327	Loma	(Prümers and Jaimes Betancourt, 2014)[11]
Loma Mendoza	1077 ± 28	895-1030	Bln-5325	Loma	(Prümers and Jaimes Betancourt, 2014)[11]
Loma Mendoza	1065 ± 29	900-1035	Bln-5214	Loma	(Prümers and Jaimes Betancourt, 2014)[11]
Loma Mendoza	1050 ± 31	900-1120	Bln-5212	Loma	(Prümers and Jaimes Betancourt, 2014)[11]
Loma Mendoza	1043 ± 43	895-1155	Erl-3201	Loma	(Prümers and Jaimes Betancourt, 2014)[11]
Loma Mendoza	1036 ± 39	905-1155	Bln-5344	Loma	(Prümers and Jaimes Betancourt, 2014)[11]
Loma Mendoza	1030 ± 28	985-1145	Bln-5211	Loma	(Prümers and Jaimes Betancourt, 2014)[11]
Loma Mendoza	1026 ± 43	970-1155	Erl-3208	Loma	(Prümers and Jaimes Betancourt, 2014)[11]
Loma Mendoza	973 ± 45	1010-1185	Erl-3200	Loma	(Prümers and Jaimes Betancourt, 2014)[11]
Loma Mendoza	961 ± 24	1030-1155	Bln-5345	Loma	(Prümers and Jaimes Betancourt, 2014)[11]
Loma Mendoza	953 ± 38	1020-1185	Erl-3203	Loma	(Prümers and Jaimes Betancourt, 2014)[11]
Loma Mendoza	950 ± 29	1025-1170	Bln-5326	Loma	(Prümers and Jaimes Betancourt, 2014)[11]
Loma Mendoza	948 ± 29	1025-1170	Bln-5213	Loma	(Prümers and Jaimes Betancourt, 2014)[11]
Loma Mendoza	651 ± 34	1285-1385	Erl-4791	Loma	(Prümers and Jaimes Betancourt, 2014)[11]
Loma Mendoza	631 ± 29	1290-1395	Bln-5210	Loma	(Prümers and Jaimes Betancourt, 2014)[11]
Loma Mendoza	609 ± 46	1285-1400	Erl-3199	Loma	(Prümers and Jaimes Betancourt, 2014)[11]
Loma Palmazola	740 ± 60	1215-1395	SI-4048	Loma	(Dougherty and Calandra, 1984)[44]
Loma Palmazola	675 ± 70	1240-1410	SI-4113	Loma	(Dougherty and Calandra, 1984)
Loma Salvatierra	1623 ± 30	465-585	KIA-31856	Loma	(Prümers and Jaimes Betancourt, 2014)[11]
Loma Salvatierra	1489 ± 27	550-645	KIA-32720	Loma	(Prümers and Jaimes Betancourt, 2014)[11]
Loma Salvatierra	1389 ± 30	620-765	Bln-5945-L	Loma	(Prümers and Jaimes Betancourt, 2014)[11]
Loma Salvatierra	1380 ± 65	560-855	SI-5391	Loma	(Prümers and Jaimes Betancourt, 2014)[11]
Loma Salvatierra	1350 ± 20	650-765	KIA-31854	Loma	(Prümers and Jaimes Betancourt, 2014)[11]
Loma Salvatierra	1341 ± 24	650-770	KIA-31855	Loma	(Prümers and Jaimes Betancourt, 2014)[11]
Loma Salvatierra	1337 ± 39	650-770	Bln-5860	Loma	(Prümers and Jaimes Betancourt, 2014)[11]
Loma Salvatierra	1335 ± 26	655-770	KIA-38804	Loma	(Prümers and Jaimes Betancourt, 2014)[11]
Loma Salvatierra	1325 ± 50	645-865	SI-5393	Loma	(Prümers and Jaimes Betancourt, 2014)[11]
Loma Salvatierra	1316 ± 27	665-770	KIA-38803	Loma	(Prümers and Jaimes Betancourt, 2014)[11]
Loma Salvatierra	1311 ± 26	670-770	Bln-5861	Loma	(Prümers and Jaimes Betancourt, 2014)[11]
Loma Salvatierra	1300 ± 23	675-770	KIA-38805	Loma	(Prümers and Jaimes Betancourt, 2014)[11]
Loma Salvatierra	1278 ± 53	665-885	Erl-8016	Loma	(Prümers and Jaimes Betancourt, 2014)[11]

Loma Salvatierra	1275 ± 39	675-875	Bln-5947 LI	Loma	(Prümers and Jaimes Betancourt, 2014)[11]
Loma Salvatierra	1275 ± 46	675-880	Erl-8014	Loma	(Prümers and Jaimes Betancourt, 2014)[11]
Loma Salvatierra	1240 ± 28	710-890	KIA-38802	Loma	(Prümers and Jaimes Betancourt, 2014)[11]
Loma Salvatierra	1239 ± 31	690-890	KIA-32718	Loma	(Prümers and Jaimes Betancourt, 2014)[11]
Loma Salvatierra	1228 ± 23	765-885	KIA-38813	Loma	(Prümers and Jaimes Betancourt, 2014)[11]
Loma Salvatierra	1224 ± 24	770-890	KIA-38808	Loma	(Prümers and Jaimes Betancourt, 2014)[11]
Loma Salvatierra	1223 ± 26	765-895	KIA-38812	Loma	(Prümers and Jaimes Betancourt, 2014)[11]
Loma Salvatierra	1201 ± 24	770-950	KIA-32719	Loma	(Prümers and Jaimes Betancourt, 2014)[11]
Loma Salvatierra	1156 ± 25	870-990	KIA-31858	Loma	(Prümers and Jaimes Betancourt, 2014)[11]
Loma Salvatierra	1105 ± 80	765-1155	SI-5394	Loma	(Prümers and Jaimes Betancourt, 2014)[11]
Loma Salvatierra	1060 ± 25	970-1030	KIA-38800	Loma	(Prümers and Jaimes Betancourt, 2014)[11]
Loma Salvatierra	1044 ± 44	895-1155	Erl-8012	Loma	(Prümers and Jaimes Betancourt, 2014)[11]
Loma Salvatierra	1041 ± 20	985-1030	KIA-31859	Loma	(Prümers and Jaimes Betancourt, 2014)[11]
Loma Salvatierra	1040 ± 45	895-1155	SI-5878	Loma	(Prümers and Jaimes Betancourt, 2014)[11]
Loma Salvatierra	1035 ± 95	775-1220	SI-5390	Loma	(Prümers and Jaimes Betancourt, 2014)[11]
Loma Salvatierra	1030 ± 44	905-1155	Erl-8013	Loma	(Prümers and Jaimes Betancourt, 2014)[11]
Loma Salvatierra	1007 ± 22	995-1150	KIA-38810	Loma	(Prümers and Jaimes Betancourt, 2014)[11]
Loma Salvatierra	1005 ± 50	975-1175	SI-5879	Loma	(Prümers and Jaimes Betancourt, 2014)[11]
Loma Salvatierra	985 ± 45	990-1170	Erl-8015	Loma	(Prümers and Jaimes Betancourt, 2014)[11]
Loma Salvatierra	957 ± 23	1030-1155	KIA-38801	Loma	(Prümers and Jaimes Betancourt, 2014)[11]
Loma Salvatierra	956 ± 25	1030-1160	KIA-31857	Loma	(Prümers and Jaimes Betancourt, 2014)[11]
Loma Salvatierra	948 ± 25	1030-1165	KIA-32717	Loma	(Prümers and Jaimes Betancourt, 2014)[11]
Loma Salvatierra	947 ± 21	1035-1165	KIA-38807	Loma	(Prümers and Jaimes Betancourt, 2014)[11]
Loma Salvatierra	932 ± 22	1040-1185	KIA-38809	Loma	(Prümers and Jaimes Betancourt, 2014)[11]
Loma Salvatierra	896 ± 32	1040-1230	KIA-38814	Loma	(Prümers and Jaimes Betancourt, 2014)[11]
Loma Salvatierra	820 ± 70	1045-1300	SI-5392	Loma	(Prümers and Jaimes Betancourt, 2014)[11]
Loma Salvatierra	740 ± 23	1260-1300	KIA-38811	Loma	(Prümers and Jaimes Betancourt, 2014)[11]
Loma Salvatierra	596 ± 22	1300-1355	KIA-38806	Loma	(Prümers and Jaimes Betancourt, 2014)[11]

Supplementary Table 6. Radiocarbon dates for Xinguano sites in Southern Amazon.

Southern Amazon					
Site	Date (RCYBP)	cal CE (2σ)	Laboratory#	Phase	Reference
MT-FX-06	1030 ± 60	965-1175	Beta-176141	Pre-Earthwork	(Heckenberger et al., 2008)[46]
MT-FX-06	1000 ± 70	970-1185	Beta-72261	Pre-Earthwork	(Heckenberger, 2005)[12]
MT-FX-06	700 ± 70*	1220-1410	Beta-78979	Pre-Earthwork	(Heckenberger, 2005)[12]
MT-FX-06	750 ± 40	1235-1390	Beta-194843	Xinguano Fortification	(Heckenberger et al., 2008)[46]
MT-FX-06	720 ± 40	1260-1395	Beta-194841	Xinguano Fortification	(Heckenberger et al., 2008)[46]
MT-FX-06	710 ± 50	1265-1400	Beta-176136	Xinguano Fortification	(Heckenberger et al., 2008)[46]
MT-FX-06	700 ± 50	1270-1400	Beta-194840	Xinguano Fortification	(Heckenberger et al., 2008)[46]
MT-FX-06	590 ± 60	1295-1440	Beta-176139	Xinguano Fortification	(Heckenberger, 2005)[12]
MT-FX-06	530 ± 60	1305-1480	Beta-176140	Xinguano Fortification	(Heckenberger, 2005)[12]
MT-FX-06	440 ± 60	1400-1610	Beta-176135	Xinguano Fortification	(Heckenberger, 2005)[12]
MT-FX-06	440 ± 70	1395-1610	Beta-72262	Xinguano Fortification	(Heckenberger, 2005)[12]
MT-FX-06	360 ± 70	1420-1600	Beta-81301	Xinguano Fortification	(Heckenberger, 2005)[12]
MT-FX-06	340 ± 60	1435-1600	Beta-176137	Xinguano Fortification	(Heckenberger, 2005)[12]
MT-FX-06	180 ± 60*	1650-1950	Beta-72260	Xinguano Fortification	(Heckenberger, 2005)[12]
MT-FX-07	680 ± 70	1280-1440	GIF-5365	Xinguano Fortification	(Becquelin, 1993)[47]
MT-FX-07	600 ± 80	1265-1415	GIF-3307	Xinguano Fortification	(Becquelin, 1993)[47]
MT-FX-11	900 ± 60	1035-1265	Beta-72262	Pre-Earthwork	(Heckenberger, 2005)[12]
MT-FX-11	440 ± 70	1395-1640	Beta-72263	Xinguano Fortification	(Heckenberger, 2005)[12]
MT-FX-13	910 ± 80	1010-1205	Beta-88363	Pre-Earthwork	(Heckenberger et al., 1999)[34]
MT-FX-13	930 ± 50	1050-1225	Beta-197516	Xinguano Fortification	(Heckenberger et al., 2008)[46]
MT-FX-13	890 ± 40	1050-1230	Beta-197515	Xinguano Fortification	(Heckenberger et al., 2008)[46]
MT-FX-13	690 ± 60*	1235-1410	Beta-88362	Xinguano Fortification	(Heckenberger et al., 1999)[34]

Supplementary Table 7. Sites used in the composition of the regional charcoal curves. Methods: SIEV = sieved, HNPK = handpicked, POLS = pollen slide, IMAG = charcoal particles identified by imaging software

Region	Site	Lat	Long	Age range (est. BP)	N. dates	N. samples	Method	References
Llanos de Moxos	Laguna Chaplin	-14.4667	-61.0667	24482 to 73	14	31	SIEV	(Burbridge et al., 2017; Mayle et al., 2000)[48,49]
Llanos de Moxos	Laguna Bella Vista	-13.6167	-61.5500	19918 to -55	15	38	SIEV	(Burbridge et al., 2017; Mayle et al., 2000)[48,49]
Llanos de Moxos	Pontes e Lacerda	-15.2667	-59.2167	9778 to -40	8	29	HNPK	(Gouveia et al., 2002)[50]
Llanos de Moxos	Pimenta Bueno	-11.8166	-61.1666	7123 to 139	3	16	SIEV	(Pessenda et al., 1998)[51]
Llanos de Moxos	Laguna Yaguarú	-15.6000	-63.2167	7830 to -55	11	50	POLS	(Taylor et al., 2010)[52]

Llanos de Moxos	Cuatro Vientos	-14.5322	-61.1307	25000 to -46	9	50	SIEV	(Maezumi et al., 2017)[53]
Llanos de Moxos	Laguna Granja	-13.2626	-63.7099	6000 to -64	5	206	SIEV	(Carson et al., 2014)[54]
Llanos de Moxos	Laguna Oricore	-13.3363	-63.5238	5680 to -64	3	82	SIEV	(Carson et al., 2014)[54]
Llanos de Moxos	Huanchaca Mesetta	-14.5549	-60.7431	14500 to -45	7	805	SIEV	(Maezumi et al., 2015)[55]
Llanos de Moxos	Lago Rogaguado	-13.0093	-65.9398	8100 to -62	7	47	SIEV	(Brugger et al., 2016)[56]
Llanos de Moxos	Lake Chalalan	-14.4278	-67.9208	16289 to 292	9	44	IMAG	(Urrego, 2006)[57]
Llanos de Moxos	Lake Santa Rosa	-14.4769	-67.8747	16086 to 64	6	84	IMAG	(Urrego, 2006)[57]
SW Amazon	Lake Werth	-11.7470	-69.2336	3303 to 0	5	86	IMAG	(Bush et al., 2007b)[58]
SW Amazon	Lake Gentry	-12.1773	-69.0977	8387 to 0	5	137	IMAG	(Bush et al., 2007b)[58]
SW Amazon	Lake Parker	-12.1406	-69.0215	12769 to 0	5	236	IMAG	(Bush et al., 2007b)[58]
SW Amazon	Lake Vargas	-12.3725	-68.8992	8036 to 50	6	25	IMAG	(Bush et al., 2007b)[58]
SW Amazon	Porto Velho	-8.3500	-63.9500	20418 to 66	5	16	SIEV	(De Freitas et al., 2001)[59]
E Amazon	Lake Tapera	0.1300	-51.0777	8060 to -49	6	40	SIEV	(De Toledo and Bush, 2007)[60]
E Amazon	Lake Marcio	0.1638	-51.0624	7250 to -49	6	39	SIEV	(De Toledo and Bush, 2007)[60]
E Amazon	Lago Caranã	-2.8356	-55.0425	8500 to -64	16	448	SIEV	(Maezumi et al., 2018)[31]
E Amazon	Lake Comprida	-1.6249	-53.9996	13209 to -50	7	23	POLS	(Bush et al., 2000)[61]
E Amazon	Lake Geral	-1.6469	-53.5955	8304 to 87	3	70	IMAG	(Bush et al., 2000)[61]
E Amazon	Lago Crispim	-0.6226	-47.6436	7608 to -10	4	41	POLS	(Behling and Lima da Costa, 2001)[62]
E Amazon	Rio Curua	-1.7347	-51.4549	7528 to 51	6	36	POLS	(Behling and da Costa, 2000)[63]
E Amazon	Lagoa da Curuça	-0.7667	-47.8500	15765 to -24	5	25	POLS	(Behling, 2001)[64]

E Amazon	Lake Saracuri	-1.6788	-53.5703	8486 to 10	6	86	POLS	(Bush et al., 2007a)[65]
E Amazon	Lake Santa Maria	-1.5783	-53.6054	11491 to 18	6	89	IMAG	(Bush et al., 2007a)[65]
E Amazon	Lago Tapajós	-2.7758	-55.0828	12432 to 223	6	18	POLS	(Bush et al., 2007a)[65]

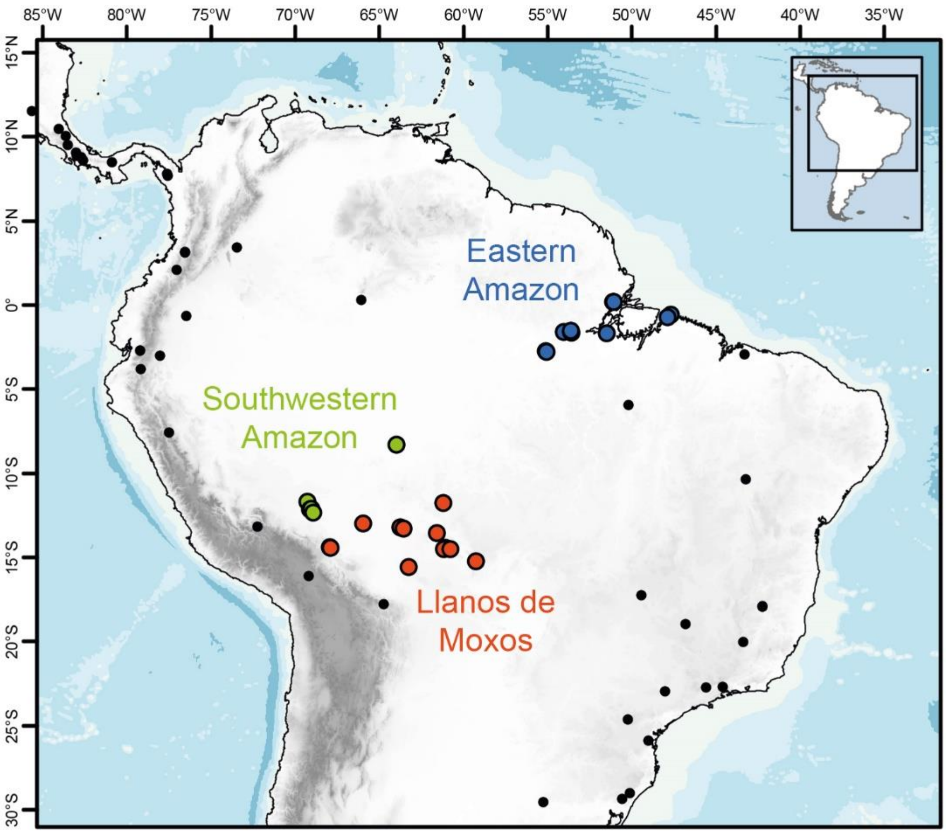

Supplementary Figure 1. Sites used in the compilation of the RCCs (Supplementary Table 7) and other charcoal records from South America (compiled from the Global Charcoal Database: https://www.paleofire.org/).

Supplementary Methods

Sum of the Calibrated Probability Distributions (SPDs): The SPDs are a standard method for representing chronological trends in radiocarbon data sets. SPDs are produced by calibrating each independent date in the sample and adding the results to produce a single density distribution[66,67]. This has the advantage of including the full range of probabilities associated with calibrated dates, instead of using single point estimates. SPDs were built in R using the *spd* function of the *rcarbon* package[67-69] and the unnormalised, calibrated dates from each analysed region (Supplementary Tables 1-6). To account for oversampling of some sites and phases within those sites, we applied a binning procedure[67]. Dates within sites were ordered and those occurring within 200 years of each other were grouped into bins using the *binPrep* function.

Regional charcoal curves: To investigate potential natural and anthropogenic drivers of palaeofire (past fire activity), existing charcoal records were compiled into composite regional charcoal curves

(RCCs)[70,71] to reconstruct changes in regional scale biomass burning. As a result of the paucity of charcoal records across Amazonia, all charcoal records in existence across the six study regions were included. Three of the areas had charcoal data available: the eastern Amazon, the southwestern Amazon, and the Llanos de Moxos (Supplementary Table 7, Supplementary Figure 1). RCCs were created for each of these regions and compared with cultural and climate data. In the latter case, they could be used as further proxies for changes in human activity, cultural phases and subsistence strategies considering what is known about pre-Columbian land use in each region. It is expected that changes in fire activity that do not coincide with climate trends (increase or decrease in precipitation) are better explained as resulting from human activity.

To examine regional biomass burning during the late Holocene, charcoal records were compiled from the Global Charcoal Database (GCD version 2.0), recently published charcoal records[31,56] and records in the regions not included in the database (e.g. [60]). A total of 29 charcoal records were included and analyzed using the paleofire R package software (version 1.1.8)[72]. Charcoal records used in this study were compiled from the GCD ver 2.0 and recently published records in the study areas selected for this study. Records that had greater than 16 samples were included in the 3 regional charcoal curves. See Supplementary Table 7 for details. Based of the available charcoal records, three RCCs were created in the eastern Amazon, the Llanos de Moxos and the southwestern Amazon. For the eastern Amazon, 11 charcoal records between 0°S and 2°N and 47°W to 55°W were included in the RCC, in the southwestern Amazon, five charcoal records were included in the RCC between 8°S and 12°S and 63°W to 69°W, and in the Llanos de Moxos, 12 charcoal records between 11°S and 15°S and 59°W to 61°W were used (Supplementary Table 7, Supplementary Figure 1). To facilitate inter-site comparison, all records are pretreated using standard protocol for transforming and standardizing individual records, which includes: (1) transforming non-influx data (e.g., concentration particles cm^{-3}) to influx values (particle cm^{-2} yr^{-1}), (2) homogenizing the variance using the Box-Cox transformation, (3) rescaling the values using a minimax transformation to allow comparisons among sites, and (4) rescaling the values to z-scores using a base period of 200 years[70,71]. Sites are smoothed with a 200 year half-width smoothing window and a bootstrap of 1000 years[72].

Supplementary References

1 Neves, E. in *Ethnicity in Ancient Amazonia: Reconstructing Past Identities from Archaeology, Linguistics, and Ethnohistory* (eds A. Hornborg & J.D. Hill) 31-56 (University of Colorado Press, 2011).

2 Rostain, S. in *Handbook of South American Archaeology* (eds H. Silverman & W. H Isbell) 279-302 (Springer, 2008).

3 Schaan, D. P. in *The Handbook of South American Archaeology* (eds Helaine Silverman & William H. Isbell) 339-357 (Springer New York, 2008).

4 Gomes, D. M. C. Politics and Ritual in Large Villages in Santarém, Lower Amazon, Brazil. *Cambridge Archaeological Journal* **27**, 275-293, doi:10.1017/S0959774316000627 (2016).

5 Schaan, D. P. in *Beyond Waters: Archaeology and environmental history of the Amazonian Inland* (ed P. D. Stenborg) 23-36 (University of Gothenburg, 2016).

6 Moraes, C. d. P. & Neves, E. G. O ano 1000: adensamento populacional, interação e conflito na Amazônia Central. *Amazônica-Revista de Antropologia* **4**, 122-148 (2012).

7 Saunaluoma, S. in *Cerâmicas arqueológicas da Amazônia: rumo a uma nova síntese* (eds Cristiana Barreto, Helena P. Lima, & Carla J. Betancourt) 429-434 (IPHAN, 2016).

8 Saunaluoma, S. & Schaan, D. Monumentality in Western Amazonian formative societies: geometric ditched enclosures in the Brazilian state of Acre. *Antiqua* **2**, 1 (2012).

9 Saunaluoma, S. Pre-Columbian earthworks in the Riberalta region of the Bolivian Amazon. *Amazônica-Revista de Antropologia* **2** (2010).
10 Betancourt, C. J. in *Cerâmicas Arqueológicas da Amazônia: rumo a uma nova síntese* (eds C. Barreto, H. Lima, & Carla J. Betancourt) 465-477 (IPHAN, 2016).
11 Prümers, H. & Jaimes Betancourt, C. 100 años de investigación arqueológica en los Llanos de Mojos. *Arqueoantropológicas* **4**, 11-54 (2014).
12 Heckenberger, M. J. *The ecology of power: culture, place, and personhood in the southern Amazon, A.D. 1000-2000*. (Routledge, 2005).
13 Schneider, T., Bischoff, T. & Haug, G. H. Migrations and dynamics of the intertropical convergence zone. *Nature* **513**, 45, doi:10.1038/nature13636 (2014).
14 Flantua, S. G. A. *et al.* Climate variability and human impact in South America during the last 2000 years: synthesis and perspectives from pollen records. *Clim. Past* **12**, 483-523, doi:10.5194/cp-12-483-2016 (2016).
15 Wang, X. *et al.* Wet periods in northeastern Brazil over the past 210 kyr linked to distant climate anomalies. *Nature* **432**, 740, doi:10.1038/nature03067

https://www.nature.com/articles/nature03067#supplementary-information (2004).
16 Novello, V. F. *et al.* Two Millennia of South Atlantic Convergence Zone Variability Reconstructed From Isotopic Proxies. *Geophys Res Lett* **0**, doi:doi:10.1029/2017GL076838 (2018).
17 Bronk Ramsey, C. & Lee, S. Recent and planned developments of the program OxCal. *Radiocarbon* **55**, 720-730 (2013).
18 Reimer, P. J. *et al.* Intcal13 and Marine13 Radiocarbon Age Calibration Curves 0–50,000 Years Cal BP. *Radiocarbon* **55**, 1869-1887 (2013).
19 Hogg, A. G. *et al.* Shcal13 Southern Hemisphere Calibration, 0-50,000 Years Cal Bp. *Radiocarbon* **55**, 1889-1903 (2013).
20 Marsh, E. J. *et al.* IntCal, SHCal, or a Mixed Curve? Choosing a 14C Calibration Curve for Archaeological and Paleoenvironmental Records from Tropical South America. *Radiocarbon* **60**, 925-940, doi:10.1017/RDC.2018.16 (2018).
21 Bronk Ramsey, C. Bayesian analysis of radiocarbon dates. *Radiocarbon* **51**, 337-360 (2009).
22 Van den Bel, M. *Archaeological investigations between Cayenne Island and the Maroni River: a cultural sequence of western coastal French Guiana from 5000 BP to present*. (Sidestone Press, 2015).
23 Rostain, S. *L'occupation amérindienne ancienne du littoral de Guyane*. (ORSTOM Éditions, 1994).
24 McKey, D. *et al.* Pre-Columbian Agricultural Landscapes, Ecosystem Engineers and Self-organized Patchiness in Amazonia. *Proceedings of the National Academy of Sciences* **107**, 7823-7828 (2010).
25 Van den Bel, M. in *Arqueologia Amazônica* (eds E. Pereira & V. Guapindaia) 61-93 (Museu Paraense Emilio Goeldi, 2010).
26 Rouse, I. & Allaire, L. in *Chronologies in New World Archaeology* (eds Royal E. Taylor & Clement Meighan) 431-481 (Academic Press, 1978).
27 Martins, C. M. P. Sobre contatos e fronteiras: Um enfoque arqueológico. *Amazônica - Revista de Antropologia* **4**, 150-184 (2012).
28 Schaan, D. P. *The Camutins Chiefdom: Rise and Development of Social Complexity on Marajó Island, Brazilian Amazon*, University of Pittsburgh, (2004).
29 Roosevelt, A. C. *Moundbuilders of the Amazon: geophysical archaeology on Marajo Island, Brazil*. (Academic Press, 1991).
30 Meggers, B. J. & Danon, J. Identification and Implications of A Hiatus in the Archeological Sequence on Marajó Island, Brazil. *Journal of the Washington Academy of Sciences* **78**, 245-253 (1988).

31 Maezumi, S. Y. *et al.* The legacy of 4,500 years of polyculture agroforestry in the eastern Amazon. *Nature Plants* **4**, 540-547 (2018).

32 Alves, D. T. *Ocupação indígena na foz do rio Tapajós (3260-960 AP): estudo do sítio Porto de Santarém, baixo Amazonas*, Universidade Federal do Pará, (2012).

33 Quinn, E. *Excavating "Tapajó" ceramics at Santarém: their age and archaeological context* PhD thesis, University of Illinois at Chicago, (2004).

34 Heckenberger, M. J., Petersen, J. B. & Neves, E. G. Village size and permanence in Amazonia: two archaeological examples from Brazil. *Latin American Antiquity* **10**, 353-376 (1999).

35 Moraes, C. d. P. *Arqueologia na Amazônia Central vista de uma perspectiva da região do Lago do Limão*, University of São Paulo, (2006).

36 Moraes, C. d. P. *Amazônia Ano 1000: Territorialidade e Conflito no Tempo das Chefias Regionais*, University of São Paulo, (2013).

37 Arroyo-Kalin, M. in *Amazonian Dark Earths: Wim Sombroek's Vision* (eds W.I. Woods *et al.*) 33-83 (Springer, 2009).

38 Machado, J. S. *Montículos artificiais na Amazônia Central: um estudo de caso do sítio Hatahara*, University of São Paulo, (2005).

39 Prestes-Carneiro, G., Béarez, P., Bailon, S., Rapp Py-Daniel, A. & Neves, E. G. Subsistence fishery at Hatahara (750–1230 CE), a pre-Columbian central Amazonian village. *Journal of Archaeological Science: Reports* **8**, 454-462, doi:https://doi.org/10.1016/j.jasrep.2015.10.033 (2016).

40 Neves, E. G. & Petersen, J. B. in *Time and complexity in historical ecology: studies in the neotropical lowlands* (eds William Balée & Clark L. Erickson) 279–310 (Columbia University Press, 2006).

41 Schaan, D. *et al.* New radiometric dates for precolumbian (2000-700 B.P.) earthworks in western Amazonia, Brazil. *Journal of Field Archaeology* **37**, 132-142 (2012).

42 Saunaluoma, S., Pärssinen, M. & Schaan, D. Diversity of Pre-colonial Earthworks in the Brazilian State of Acre, Southwestern Amazonia. *Journal of Field Archaeology* **43**, 362-379, doi:10.1080/00934690.2018.1483686 (2018).

43 Neves, E. G. *et al.* Pesquisa e Formação nos Sítios Arqueológicos Espinhara e Sol de Campinas do Acre - PESC. (University of São Paulo, São Paulo, 2016).

44 Dougherty, B. & Calandra, H. A. Prehispanic Human Settlement in the Llanos de Moxos, Bolivia. *Quaternary of South America and Antarctic Peninsula* **2**, 163-199 (1984).

45 Erickson, C. L. in *Arqueología de las Tierras Bajas* (eds Alicia Durán Coirolo & Roberto Bracco Boksar) 207-226 (Comisión Nacional de Arqueología, 2000).

46 Heckenberger, M. J. *et al.* Pre-Columbian Urbanism, Anthropogenic Landscapes, and the Future of the Amazon. *Science* **321**, 1214-1217 (2008).

47 Becquelin, P. in *Karl von den Steinen: um século de antropologia no Xingu* (ed Vera P. Coelho) 224-232 (EDUSP, 1993).

48 Burbridge, R. E., Mayle, F. E. & Killeen, T. J. Fifty-thousand-year vegetation and climate history of Noel Kempff Mercado National Park, Bolivian Amazon. *Quaternary Research* **61**, 215-230, doi:10.1016/j.yqres.2003.12.004 (2017).

49 Mayle, F. E., Burbridge, R. & Killeen, T. J. Millennial-scale dynamics of southern Amazonian rain forests. *Science* **290**, 2291-2294 (2000).

50 Gouveia, S. E. M. *et al.* Carbon isotopes in charcoal and soils in studies of paleovegetation and climate changes during the late Pleistocene and the Holocene in the southeast and centerwest regions of Brazil. *Global and Planetary Change* **33**, 95-106, doi:https://doi.org/10.1016/S0921-8181(02)00064-4 (2002).

51 Pessenda, L. C. R. *et al.* The carbon isotope record in soils along a forest-cerrado ecosystem transect: implications for vegetation changes in the Rondonia state, southwestern Brazilian Amazon region. *The Holocene* **8**, 599-603, doi:10.1191/095968398673187182 (1998).

52 Taylor, Z. P., Horn, S. P., Mora, C. I., Orvis, K. H. & Cooper, L. W. A multi-proxy palaeoecological record of late-Holocene forest expansion in lowland Bolivia. *Palaeogeography, Palaeoclimatology, Palaeoecology* **293**, 98-107, doi:https://doi.org/10.1016/j.palaeo.2010.05.004 (2010).
53 Maezumi, S. Y., Whitney, B. S., Mayle, F. E., Gregorio de Souza, J. & Iriarte, J. Reassessing climate and pre-Columbian drivers of paleofire activity in the Bolivian Amazon. *Quaternary International*, doi:https://doi.org/10.1016/j.quaint.2017.11.053 (2017).
54 Carson, J. F. *et al.* Environmental impact of geometric earthwork construction in pre-Columbian Amazonia. *Proceedings of the National Academy of Sciences* **111**, 10497-10502 (2014).
55 Maezumi, S. Y., Power, M. J., Mayle, F. E., McLauchlan, K. K. & Iriarte, J. Effects of past climate variability on fire and vegetation in the cerrãdo savanna of the Huanchaca Mesetta, NE Bolivia. *Clim. Past* **11**, 835-853, doi:10.5194/cp-11-835-2015 (2015).
56 Brugger, S. O. *et al.* Long-term man–environment interactions in the Bolivian Amazon: 8000 years of vegetation dynamics. *Quaternary Science Reviews* **132**, 114-128, doi:https://doi.org/10.1016/j.quascirev.2015.11.001 (2016).
57 Urrego, D. *Long-term vegetation and climate change in Western Amazonia*, Florida Institute of Technology, (2006).
58 Bush, M. B., Silman, M. R. & Listopad, C. M. C. S. A regional study of Holocene climate change and human occupation in Peruvian Amazonia. *Journal of Biogeography* **34**, 1342-1356, doi:doi:10.1111/j.1365-2699.2007.01704.x (2007).
59 De Freitas, H. A. *et al.* Late Quaternary Vegetation Dynamics in the Southern Amazon Basin Inferred from Carbon Isotopes in Soil Organic Matter. *Quaternary Research* **55**, 39-46, doi:http://dx.doi.org/10.1006/qres.2000.2192 (2001).
60 De Toledo, M. B. & Bush, M. B. A mid-Holocene environmental change in Amazonian savannas. *Journal of Biogeography* **34**, 1313-1326, doi:doi:10.1111/j.1365-2699.2006.01606.x (2007).
61 Bush, M. B., Miller, M. C., De Oliveira, P. E. & Colinvaux, P. A. Two histories of environmental change and human disturbance in eastern lowland Amazonia. *The Holocene* **10**, 543-553, doi:10.1191/095968300672647521 (2000).
62 Behling, H. & Lima da Costa, M. Holocene vegetational and coastal environmental changes from the Lago Crispim record in northeastern Pará State, eastern Amazonia. *Rev Palaeobot Palyno* **114**, 145-155, doi:https://doi.org/10.1016/S0034-6667(01)00044-6 (2001).
63 Behling, H. & da Costa, M. L. Holocene Environmental Changes from the Rio Curuá Record in the Caxiuanã Region, Eastern Amazon Basin. *Quaternary Research* **53**, 369-377, doi:https://doi.org/10.1006/qres.1999.2117 (2000).
64 Behling, H. Late Quaternary environmental changes in the Lagoa da Curuça region (eastern Amazonia, Brazil) and evidence of Podocarpus in the Amazon lowland. *Veg Hist Archaeobot* **10**, 175-183 (2001).
65 Bush, M. B. *et al.* Holocene fire and occupation in Amazonia: records from two lake districts. *Philosophical Transactions of the Royal Society B: Biological Sciences* **362**, 209-218, doi:10.1098/rstb.2006.1980 (2007).
66 Shennan, S. *et al.* Regional population collapse followed initial agriculture booms in mid-Holocene Europe. *Nature Communications* **4** (2013).
67 Timpson, A. *et al.* Reconstructing regional population fluctuations in the European Neolithic using radiocarbon dates: a new case-study using an improved method. *Journal of Archaeological Science* **52**, 549-557 (2014).
68 Crema, E. R., Habu, J., Kobayashi, K. & Madella, M. Summed Probability Distribution of 14C Dates Suggests Regional Divergences in the Population Dynamics of the Jomon Period in Eastern Japan. *PLoS One* **11**, e0154809, doi:10.1371/journal.pone.0154809 (2016).

69 Crema, E. R., Bevan, A. & Shennan, S. Spatio-temporal approaches to archaeological radiocarbon dates. *Journal of Archaeological Science* **87**, 1-9, doi:https://doi.org/10.1016/j.jas.2017.09.007 (2017).
70 Marlon, J. R. *et al.* Climate and human influences on global biomass burning over the past two millennia. *Nat Geosci* **1**, 697 (2008).
71 Power, M. J. *et al.* Changes in fire regimes since the Last Glacial Maximum: an assessment based on a global synthesis and analysis of charcoal data. *Climate Dynamics* **30**, 887-907, doi:10.1007/s00382-007-0334-x (2008).
72 Blarquez, O. *et al.* paleofire: An R package to analyse sedimentary charcoal records from the Global Charcoal Database to reconstruct past biomass burning. *Computers & Geosciences* **72**, 255-261, doi:https://doi.org/10.1016/j.cageo.2014.07.020 (2014).